RSC Advances

ROYAL SOCIETY OF CHEMISTRY

www.rsc.org/advances

Table of Content (TOC) entry

Redox reactions have been found to be favoured at nanoscale confinement of solid matrices. Softening of reaction condition as well as enhancement of reaction kinetics at confined nanospaces has been demonstrated.

Communication
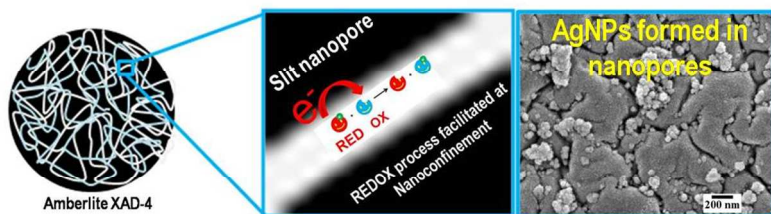
Wonderful nanoconfinement effect on redox reaction equilibrium†

**Sabyasachi Patra,[a] Ashok K. Pandey,[a] Sudip K. Sarkar,[b] A. Goswami*[a]**

Polyol and other routes of reduction of noble metal ions that are not feasible under ambient condition have been observed with appreciable rate in nanoconfined spaces of solid matrices for the first time. Also a remarkable enhancement of rate constant / activity parameter has been observed for AgNPs catalyzed BH_4^- reduction of p-nitrophenol in nanoscale confinement.

Nanoscale confinement can change the materials properties significantly with respect to bulk system, and has become interesting subject of research. Pioneering work by Turner *et al.* and Santiso *et al.* based on molecular simulation of various chemical reactions in carbon micropores shows the possibility of enhancement of reaction rates in the porous medium due to enhanced energetics.[1] This may be due to increased density of the pore phase, adsorption of some species, suitable orientation of molecules near the walls, different diffusion rates, etc in the porous medium.[1] The confinement is also known to affect catalytic behaviour of mesoporous materials.[2] In recent years, many other chemical reactions have been found to be different in nanospaces than that in a bulk system under similar conditions.[3] This enhanced reactivity is attributed to many factors like high pressure effect due to geometrical constraints,[4] shift of equilibrium towards product side because of reaction-product reduced mixing,[3a] system size dependent entropy variation[3a] etc. However, proper understanding of such effect is still limited. Recently, we showed that spaces confined to nanometer range can remarkably facilitate the redox decomposition of silver citrate complex, which is otherwise highly stable in bulk solution.[5]

Redox reactions are ubiquitous in nature and are of high importance in industry, biology as well as in geology. The reaction often takes place under vigorous conditions like high temperature and pressure. The role of nanoconfinement on redox chemical equilibrium has never been explored. In the present work, two types of nanoconfined redox reactions have been studied. These are polyol reduction of noble metal precursor ions and noble metal catalyzed reduction of p-nitrophenol with borohydride in nanopores of poly(styrene) (XAD-4) and silica gel particles (63-200 μm).

The polyol reduction process is a well established method for production of the metal nanoparticles with different aspect ratio. Generally, this process requires refluxing of a solution containing precursor ions, ethylene glycol (or other polyols) and suitable capping agent at temperature of 160 $^\circ$C or more under nitrogen/argon atmosphere.[6] The present work reports the first effort to carry out the reduction processes at room temperature by physically imposing nanoscale confinement on the reaction media with the help of nanoporous matrices. It has been observed that, during equilibration of XAD-4 beads in aqueous solution of precursor ions (Ag^+, $AuCl_4^-$, $PtCl_6^{2-}$) and ethylene glycol (EG) at room temperature (25 $^\circ$C), the colour of the beads changes to a characteristic colour of nanoparticles as shown in the representative images given in Fig.1a-d. However, no colour typical of noble metal nanoparticles has been observed in the equilibrating solution, showing absence of reduction in bulk (Fig. 1b).
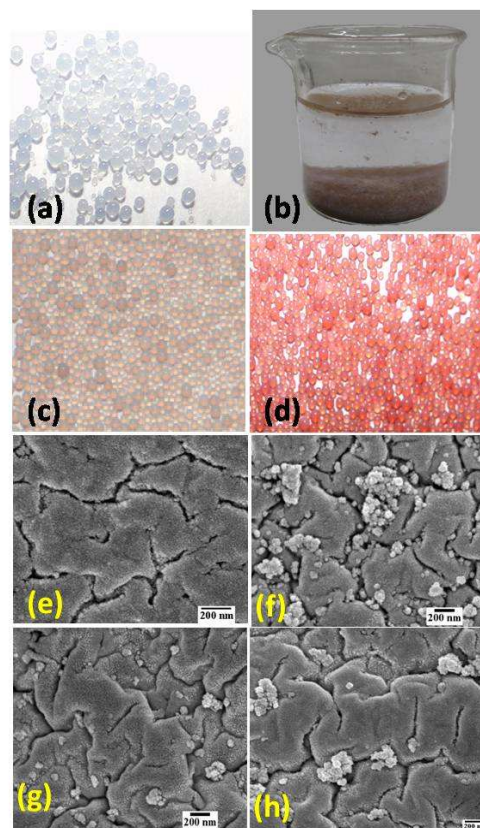
Fig. 1 Digital photograph of blank XAD-4 beads (a), XAD-4 beads equilibrated with aqueous solution of $HAuCl_4$ and EG for 48 h (b), XAD-4 beads containing AgNPs (c), XAD-4 beads containing AuNPs (d), FE-SEM image of the surface of the XAD-4 bead showing blank matrix (e), formation of silver nanoparticles (f), gold nanoparticles (g) and platinum nanoparticles (h) in the XAD-4 beads after equilibrations in aqueous solution of EG and precursor ions at room temperature for 48 h. The length of the scale bar in Fig e-h is 200 nm.

Amberlite XAD-4 spherical beads used in the present work consist of highly crosslinked macroreticular poly(styrene) having average pore diameter of 10 nm (see †ESI for details, Fig S1). It is clearly evident from the FE-SEM images given in Fig. 1f-h that the clusters of nanoparticles are seen near the nanoscale crevices in the matrix. This suggests that nanoconfinement facilitates the polyol reduction process at room temperature that is not observed in bulk solution under the same reaction condition. More images at different magnifications are given in Fig. S2-4(†ESI). It is interesting to note that the used solution containing precursor ions in EG can be stored and reused for forming nanoparticles in the beads.

It is seen from the FE-SEM image given in Fig. 2a that the clusters of small spherical Pt nanoparticles are formed after nanoconfined reduction of $PtCl_6^{2-}$ by EG at room temperature. On increasing temperature to 80 ^{o}C, the bigger sized Pt nanostructures are formed in 6 h as shown in Fig. 2b. This may be attributed to faster reduction kinetics as well as higher mobility of monomer and smaller nanoparticles. The nanoconfined reduction of $PtCl_6^{2-}$ ions was also carried out using BH_4^- ions at 80 ^{o}C for 6 h (see †ESI). In this case, uniform distributed smaller Pt nanoparticles are formed (Fig. 2c & S5). It should be noted that both EG and BH_4^- do not reduce $PtCl_6^{2-}$ ions even at 80 ^{o}C significantly in aqueous solution. Appreciable reduction of Pt ions by BH_4^- has been observed by Song *et al.*[7a] and Pal *et al.*[7b] in nanosized soft templates. Though the authors have not mentioned, the results show possible effect of nanoconfinement in facilitating the reduction.
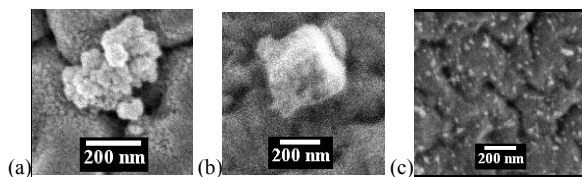

Fig. 2 FE-SEM images showing distributions of Pt nanoparticles in poly(styrene) beads after nanoconfined reduction of $PtCl_6^{2-}$ ions with EG at 25 ^{o}C (a), EG at 80 ^{o}C, (b) and BH_4^- at 80 ^{o}C (c).

It has been seen in our earlier work that the silver-citrate complexes stable in bulk aqueous solution in an excess of citrate ions ([citrate/Ag$^+$]>>1), decomposes readily in nanoconfinement of ion-exchange film or XAD-4 beads.[5] Thus, in order to study the matrix dependence of nanoconfinement effect, the method of auto-reduction of silver-citrate complex have been extended further in the nanoconfinement of silica gel particles having 4 nm pores. As shown in Fig.3, Ag nanoparticles are formed by nanoconfinement facilitated auto-reduction of silver-citrate complex in nanopores of the silica matrix, which shows that the nanoconfinement effect is matrix independent.
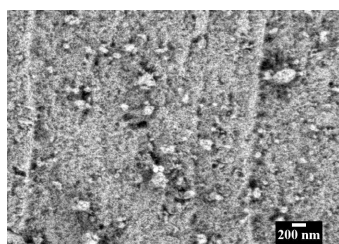

Fig. 3 The FE-SEM image showing distribution of Ag nanoparticles (brighter spots) in nanoporous silica matrix.

Thus, the selective reduction in nanoconfined spaces provides a soft synthetic route for preparing a variety of noble metal nanoparticles stabilized in inorganic or polymer matrices using an appropriate combination of reductant and precursor ions.

The reduction of p-nitrophenol (PNP) to p-aminophenol (PAP) with borohydride is thermodynamically favorable (E_0 for PNP/ PAP = -0.76 V and H_3BO_3/BH_4^- = -1.33 V versus NHE) but requires electron transfer mediated by coinage metal NPs surfaces from BH_4^- to PNP because of the presence of the kinetic barrier.[8a] Most studies have shown that AuNPs and AgNPs catalyze this reaction, and kinetics of reduction is highly dependent upon the shape, size, capping, and amount of NPs. On addition of $NaBH_4$ solution, the absorbance peak of PNP shifts immediately from 317 to 400 nm due to the formation of p-nitrophenolate anions.[8] The chemisorption of nitrophenolate anions occurs via binding through the two oxygens of the nitro group at the surface of NPs forming a pentagonal M−O−N−O−M cyclic intermediate.[9] Based on theoretical models, the binding strength of nitrophenolate with surfaces of Au and Ag NPs are expected to be similar and better than that on surfaces of other coinage metal (Cu, Pt and Pd).[9] Thus, it is expected that Au and Ag would have similar catalytic efficiency in the reduction of PNP to PAP with BH_4^- ions. Contrary to this, Gangula et al. have observed that AgNPs (K = 4.06 x 10^{-3} s^{-1}) exhibit lower catalytic rates relative to AuNPs (K = 9.19 x10^{-3} s^{-1}).[8a] This has been attributed to the lowering of reduction potential of AgNPs in the presence of strong nucleophile like BH_4^- and consequent poisoning of AgNPs surface by the formation of oxide layer.[8a] In the present work, AgNPs are stabilized in the pores of poly(styrene) matrix against such possible corrosion and easily accessible through interconnected nonopores in the matrix. Also, there is a possibility of infuencing the reduction rate by nanoconfinement effect. Therefore, the poly(styrene) beads containing Ag particles formed by EG reduction at room temperature have been tested for catalytic borohydride reduction of PNP to PAP. As seen from Fig. S6 (see †ESI), the reduction of 4-nitrophenolate anions to PAP leads to decrease in absorbance at 400 nm, and increase in absorbance at 300 nm.

It is reported in the literature that the reduction of PNP to PAP in excess of $NaBH_4$ follows pseudo-first-order kinetics that can be represented as:[8,9]

$$\ln(A_t/A_0) = - kt \qquad (1)$$

Where A_O is the absorbance representing initial concentration of PNP, A_t is the absorbance at time t and k is the catalytic reduction rate constant. It is seen from the variation of ln (A_t/A_0) as a function of time given in Fig.5 that there is a lag time in onset of the reduction process. This lag time has also been observed in other such studies.[8a,9] In the presence of excess of BH_4^- ions, the reduction of PNP is two step process i.e. (i) diffusion and chemisorption of PNP to the AgNPs, and (ii) electron transfer mediated by AgNPs surfaces from BH_4^- ions to PNP. It is seen that, after a certain lag time, ln (A_t/A_0) varies linearly with t indicating that the reduction of PNP with BH_4^- ions in the presence of Ag nanoparticles embedded poly(styrene) beads follow pseudo-first-order kinetics. As reduction proceeds, the slope changes suddenly indicating onset of unprecedented acceleration in the rate of reduction by "nanoconfinement effect".

CREATED USING THE RSC COMMUNICATION TEMPLATE (VER. 2.1) - SEE WWW.RSC.ORG/ELECTRONICFILES FOR DETAILS   **RSC Advances**   **Page 4 of 4**

ARTICLE TYPE   www.rsc.org/xxxxxx | XXXXXXXX

The delay in observing "nanoconfinement effect" may be associated to steady state diffusion of reactants in the interconnected nanopores containing AgNPs to augment the reduction process occurring at the exterior matrix.
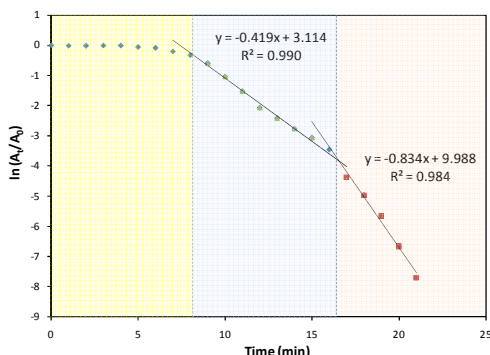

Fig. 5 Variation of logarithm of A_t/A_0 as a function of time during reduction of PNP to PAP in presence of poly(styrene) beads containing Ag nanoparticles formed by nanoconfined reduction with EG. A_t and A_0 represents absorbance of 400 nm at time t and initial, respectively.

Table 1. Comparison of rate constant (k) and activity parameter (κ) of some AgNP catalysts during BH_4^- reduction of PNP at room temperature.

nanoparticles	k (s^{-1})	$κ$ $(s^{-1} g^{-1})$	ref
Biogenic AgNP	4.06×10^{-3}	-----	8a
AgNP aggregates	2.1×10^{-3}	2.0	8b
Ag-C	1.69×10^{-3}	1.69	8c
Ag dendrite (coral like)	5.19×10^{-3}	1.30	8d
Ag dendrite (banana leaf like)	1.65×10^{-3}	0.41	8d
AgNP spherical	3.64×10^{-4}	0.09	8d
AgNP @ cationic polystyrene bead	$^a5.27 \times 10^{-3}$	$^b107.5$	8e
AgNP @ neutral nanoporous polystyrene bead (XAD-4)	13.9×10^{-3}	$^b974.07$	this work

^{a}data obtained at 30 ^oC.
^{b}rate constant per unit mass of silver only.

The values of rate constant k have been calculated from the slopes of linear portions of curve given in Fig.5. The value of first k has been found to be 6.98×10^{-3} s^{-1} with an activity parameter κ = 489.13 $s^{-1}g^{-1}$ (rate constant per unit mass of silver). The silver loading in our case has been determined by ICP-AES technique (see †ESI) and has been found to be 0.143 mg per g of XAD beads. Jana *et al.* have studied the catalytic acitivity of AgNPs, embedded in cationic polystyrene beads (SERALITE-SRA-400), which is chemically most similar to our system.[8e] The difference is in the charge and morphology of the beads. They have reported the rate constant $k = 5.27 \times 10^{-3}$ s^{-1}. The activity parameter κ (rate constant per unit mass of Ag) in their case has been found to be 107.5 $s^{-1}g^{-1}$, which is higher than free AgNPs systems.[8a-d] The value of activity parameter (κ) obtained with silver nanoprticles embedded in nanopores of the poly(styrene) beads is significantly higher than values reported by Jana *et al.* The final value of k obtained from second slope is found to be 13.9×10^{-3} s^{-1} with an activity parameter of 974.07 $s^{-1}g^{-1}$. This is remarkable considering the fact that the reduction rate in the present case involve diffusion of PNP in poly(styrene) matrix. This seems to suggest

that nanoconfinement may also be enhancing Ag catalyzed reduction of PNP in the nanopores of poly(styrene). It is noteworthy that, the higher value of activity parameter (κ) in the work reported by Jana *et al.* in comparison to bare AgNPs may also be attributed to the possible confinement effect by the porous resin beads, which has not been explored by them.

In conclusion, the redox reactions are remarkably facilitated in nanoconfined spaces. This concept of nanoconfinement effect may open a new domain of studying various redox reactions in confined nanospaces having commercial and technological importance.

Notes and references

^{a}*Radiochemistry Division & ^{b}GAM Division, Bhabha Atomic Research Centre, Trombay, Mumbai 400 085, India. Fax: +91-22-25505151; Tel: +91-22-25593688; E-mail: agoswami@barc.gov.in.*

1   (a) C.H. Turner, J.K. Johnson, KE. Gubbins, *J. Chem. Phys*., 2001, **114**, 1851-1859; (b) C.H. Turner, J.K. Brennan, J.K. Johnson, K.E. Gubbins, *J. Chem. Phys*., 2002, **116**, 2138-2148; (c) E.E. Santiso, A.M. George, M. Sliwinska-Bartkowiak, M.B. Nardelli, K.E. Gubbins, *Adsorption*, 2005, **11**, 349-354.
2   F. Goettmanna, C.Sanchez, *J. Mater. Chem*., 2007, **17**, 24–30.
3   (a) M. Polak, L. Rubinovich, *Nano Lett.,* 2008, **8**, 3543-3547; (b) M. Polak, L. Rubinovich, *Phys. Chem. Chem. Phys.,* 2011, **13**, 16728-16734; (c) L. Rubinovich, M. Polak, *Nano Lett.*, 2013, **13**, 2247-2251; (d) T. K. Nielsen, U. Bosenberg, R. Gosalawit, M. Dornheim, Y. Cerenius, F. Besenbacher, T. R. Jensen, *ACS Nano,* 2010, **4**, 3903-3908; (e) S. Li, W. H. Thompson, *J. Phys. Chem. B*. 2005, **109**, 4941-4946; (f) W. H. Thompson, *J. Chem. Phys.,* 2002, **117**, 6618-6628; (g) T. L. Hill, *Nano Lett.,* 2001,**1**, 273-275.
4   Y. Long, J. C. Palmer, B. Coasne, M. Sliwinska-Bartkowiak, G. Jackson, E. A. Müller, K. E. Gubbins, *J. Chem. Phys.* 2013, **139**, 144701-144712.
5   S. Patra, A. K. Pandey, D. Sen, S. V. Ramagiri, J. R. Bellare, S. Mazumder, A. Goswami, *Langmuir,* 2014, **30**, 2460−2469.
6   (a) S. Ayyappan, G.N. Subbanna, R.S. Gopalan, C.N.R. Rao, *Solid State Ionics* 1996, **84**, 271-281; (b) C. Chen, L. Wang, H. Yu, G. Jiang, Q. Yang, J. Zhoua, W. Xiang, J. Zhang, *Materials Chemistry and Physics*, 2008, **107**, 13–17; (c) S.J. Cho, A. Suri, X. Mei, J. Ouyang. *RSC Adv*., 2013, **3**, 1201–1209; (d) Y. Sun, B. Gates, B. Mayers, Y. Xia. *Nano Lett.,* 2002, **2**, 165-168; (e) R. Kasuya, J. Balachandran, T. Itoh, T. Matsumoto. Abstract No. C4.10. 2010, Abstract Viewer. San Francisco, CA: Materials Research Society; (f) J. Yin, J. Wang, M. Li, C. Jin, T. Zhang, *Chem. Mater*., 2012, **24**, 2645−2654.
7   (a) Y. Song, R.M. Garcia, R.M. Dorin, H. Wang, Y. Qiu, E.N. Coker, W.A. Steen, J.E. Miller, J.A. Shelnutt, *Nano Lett*., 2007, **7 (12)**, 3650-3655; (b) A. Pal, S. Shah, S. Belochapkine, D. Tanner, E. Magner, S. Devi, *Colloids and Surfaces A: Physicochem. Eng. Aspects*, 2009, **337**, 205–207.
8   (a) A. Gangula, R. Podila, M. Ramakrishna, L. Karanam, C. Janardhana, A. M. Rao, *Langmuir*, 2011, **27**, 15268-15274. (b) Y. Liu, Y. Zhang, H. Ding, S. Xu, M. Li, F. Kong, Y. Luo, G. Li, *J. Mater. Chem. A*, 2013, **1,** 3362-3371. (c) S. Tang, S. Vongehr, X. Meng, *J. Mater. Chem*., 2010, **20**, 5436-5445. (d) M. H. Rashid, T. K. Mandal, *J. Phys. Chem. C*, 2007, **111**, 16750-16760. (e) S. Jana, S. K. Ghosh, S. Nath, S. Pande, S. Praharaj, S. Panigrahi, S. Basu, T. Endo, T. Pal, *Applied Catalysis A: General*, 2006, **313**, 41-48.
9   Z.D. Pozun, S.E. Rodenbusch, E. Keller, K. Tran, W. Tang, K. J. Stevenson, G. Henkelman, *J. Phys. Chem. C*, 2013, **117**, 7598−7604.